

Spin-orbit interaction in InAs/AlSb/GaSb heterostructures quantified by weak antilocalization

F. Herling^{1,2}, C. Morrison^{1,3}, C.S. Knox^{1,4}, S. Zhang⁵, D. A. Ritchie⁶, O. Newell³, M. Myronov³, E.H. Linfield⁴ and C.H. Marrows¹

¹School of Physics and Astronomy, University of Leeds, Leeds, LS2 9JT, UK

²Novel Materials Group, Institut für Physik, Humboldt-Universität zu Berlin, 12489 Berlin, Germany

³Department of Physics, University of Warwick, Coventry, CV4 7AL, UK

⁴School of Electronic and Electrical Engineering, University of Leeds, Leeds, LS2 9JT, UK

⁵EPSRC National Centre for III-V Technologies, Department of Electronic and Electrical Engineering, University of Sheffield, Sheffield, UK

⁶Department of Physics, University of Cambridge, Cambridge, CB3 0HE, UK

Abstract: We study the spin-orbit interaction (SOI) in InAs/AlSb/GaSb heterostructures with varying layer thicknesses. We show through temperature and gate dependent magnetotransport measurements of weak antilocalization that the dominant spin-orbit relaxation mechanism in our low-mobility InAs/GaSb heterostructures is Elliott-Yafet and not Dyakonov-Perel in the form of the Rashba or Dresselhaus SOI as previously suggested. The SOI strength may be controlled using an electrostatic gate, opening up prospects for developing spintronic applications.

InAs/GaSb heterostructures have seen renewed research interest in recent years. Early work focussed on coupling a 2D electron gas (2DEG) in the InAs layer with a 2D hole gas in the GaSb layer, creating hybridized electron-hole quantum states [1-8]. Much later, it was predicted that a topologically insulating state could be created in an InAs/GaSb heterostructure [9] by using band inversion due to the band edge positions of the conduction and valence bands in InAs and GaSb, respectively, to create an energy gap in the bulk and counter-propagating spin-polarized edge states, known as the quantum spin Hall effect (QSHE). Shortly after this theoretical prediction the bulk topological gap was demonstrated experimentally [10], and recent research has focussed on demonstrating spin polarized edge transport and confirmation of the existence of the QSHE [11-19].

The Rashba spin-orbit interaction (SOI) has been studied in 2DEGs in several InAs and InGaAs quantum well (QW) heterostructures [20-27]. SOI gives rise to the conventional spin Hall effect (SHE), which is useful both as a means of manipulating spin in a spintronic device, whilst its inverse can be used for detecting spin-polarized currents such as those in the helical edge states generated by the QSHE. Use of the SHE to detect such helical spin states in this manner was recently achieved in an HgTe based topological insulator [28], and a similar experimental approach could be employed in the InAs/GaSb system. One of the underlying causes of spin relaxation is the Dyakonov-Perel mechanism, which originates in the spatial inversion asymmetry of the heterostructure [29]. Another contribution is momentum scattering from phonons and impurities, known as the Elliot-Yafet (EF) mechanism, owing to the mixing of spin-up and spin-down states by the SOI of the lattice ions [30]. It

is important to understand the effect of the proximity of the QWs to each other, and any induced interfacial effects, on the strength of the SOI and the relative contributions of momentum scattering (EF) and the SOIs (DP) arising from inversion asymmetry (bulk and structural).

Here we show, through magnetotransport weak antilocalization measurements of the temperature and gate dependence of the relevant scattering length scales that the dominant underlying spin relaxation mechanism in our InAs/GaSb heterostructure is EY, and not DP in form of Rashba SOI owing to structural inversion symmetry as previously suggested [21-23,25]. Furthermore, we also rule out Dresselhaus SOI, which originates in bulk inversion asymmetry, by demonstrating that the strength of the SOI may be tuned using an electrostatic gate.

We grew InAs/AlSb/GaSb heterostructures using solid source molecular beam epitaxy on (100) GaAs substrates, with varying thicknesses of the InAs and GaSb layer, and varying AlSb spacer thicknesses. A buffer of AlSb/GaAlSb was used to relax lattice mismatch strain and provide a pseudo-substrate for growth of the electrically active QW layers. The layer structure of the three heterostructures studied here are shown in figure 1; they are labelled A, B and C and are thus referred throughout.

Magnetotransport measurements were performed in the temperature range 0.3 to 1.5 K using an Oxford Instruments Heliox AC-V ^3He system with a 12T superconducting magnet, and at temperatures above 1.5 K, an Oxford Instruments ^4He flow cryostat with an 8T superconducting magnet. In all measurements, the field was applied perpendicular to the plane of the device.

Measurements were performed using a 50 μm wide and 250 μm long Hall bar geometry, fabricated by optical lithography, using 100 nm thick AuGeNi to form contacts that are Ohmic at all temperatures, and a wet etching process to define the mesa. The top gate stack comprises a 30 nm thick layer of Al_2O_3 with a 100 nm thick Cr/Au electrode. The back gate was fabricated by depositing and annealing AuGeNi on the highly doped substrate. An optical microscope image of a typical device is shown in an inset to figure 2, additionally square and Greek cross van der Pauw geometries were used. Electrical measurements were performed using an ac current excitation of 1 μA at 119.77 Hz and voltages were measured using Stanford Research Systems Model 830 lock-in amplifiers.

Figure 2 shows the magnetoresistance for wafer A, in which there is no AlSb barrier between the InAs and GaSb layers. The behaviour at low fields is characteristic of weak anti-localisation (WAL), which may be seen more clearly in the inset, with transitions to weak localisation (WL) and negative magnetoresistance above 500 mT, which suggests that a high density of impurities is present [29]. This would also explain the low mobility and high carrier density across all devices fabricated from this wafer. Other reasons for the unusual low mobility could be lattice mismatch or other interface effects. An advantage of low mobility samples lies in the distinct WAL of the magnetoresistance, which makes fitting more precise. The wafers A and B accordingly show smaller errors for the characteristic lengths than wafer C, which has a higher mobility and lower carrier density (see figure 1). A disadvantage is the damping of the Shubnikov-de Haas (SdH) oscillations for high fields, so that only one oscillation is visible and we cannot report high field SOI values through measurements of beating in the SdH oscillations, another common magnetotransport technique [21,23,25,31]. However, for certain materials the values for SOI extracted at low field from WAL are more accurate than the values deduced from high field beating in the SdH oscillations as the latter include the Zeeman effect [24] which causes additional uncertainty in the fast Fourier transform method used to determine the spin-split carrier densities [32].

Wafers B and C show the same WAL low field behaviour but opposite high field magnetoresistance (positive for the former, and negative, with two SdH oscillations, for the latter). Angular dependent measurements showed that the WAL and the Hall voltage are a sinusoidal function of the angle and

vanish for an in-plane magnetic field, which demonstrates the two-dimensional nature of the carrier confinement within the QW.

The magnetoconductivity for all wafers for different temperatures and applied gate voltages was fitted with the Hikami-Larkin-Nagaoka (HLN) model [33], which gives us three fit parameters as characteristic lengths: the SOI length, l_{SO} , which gives the average distance travelled by an electron before a flip in spin occurs, the mean free path, l_e , between elastic scattering events, and the phase coherence length, l_ϕ , between inelastic scattering events.

The fit matches the experimental data points for the low field range (between 200 and 400mT, dependent on the heterostructure) in which WAL is present, but deviates beyond that range owing to the negative (positive for wafer B) high-field magnetoresistance. The change in resistance due to WAL, i.e. the quantum correction to the conduction at low temperatures for low fields, shows a logarithmic temperature dependence (figure 3 inset), which is the expected dependence for WAL, due to the power law behaviour of the lifetimes (spin/elastic/inelastic scattering), which can be converted to the lengths reported here [34].

The temperature dependence of the three characteristic lengths for wafer A is shown in figure 4. For the lowest temperatures, a $T^{-1/2}$ behaviour is seen in phase coherence length, with a linear increase in mean free path and SOI length. For higher temperatures (above 5 K) the latter two are roughly temperature independent and the phase coherence length decreases linearly with increasing temperature. This suggests that electron-electron interactions are the dominant inelastic scattering mechanism for temperatures below ~ 5 K and that electron-phonon interaction dominates at temperatures above that [35]. The temperature independence of the elastic and SOI lengths suggests that these scattering rates are dominated by impurities, which corresponds to the analysis of the magnetoresistance data and suggests that the EY mechanism dominates in this heterostructures. The exponential drop in mean free path for the lowest temperatures is, as expected for our conclusion, paralleled by the SOI length, but cannot be explained, as, for example, a freezing out of the impurities would show an opposite trend.

The electrical properties and characteristic lengths of all three wafers at 1.7 K are listed in figure 1. The carrier density was calculated from the Hall coefficient and the majority carriers are electrons determined from the sign of the Hall coefficient. There was no evidence of band inversion for top, back or double gated devices, perhaps due to the high carrier density and low mobility, so we cannot contribute to current arguments regarding recent findings for SOI close to the charge neutrality point [36].

In accordance with our interpretation of the magnetoresistance and the temperature behaviour, a weak SOI is seen for the lowest carrier density (wafer C), which is the expected trend for the EY mechanism. But, this could also be explained by the DP mechanism, which originates in the missing inversion symmetry of the heterostructure. The dependence of SOI on intrinsic carrier density points to bulk inversion asymmetry (Dresselhaus) [29]. This wafer also shows the longest elastic and inelastic scattering lengths due to the high carrier mobility. This could be due to a lower impurity concentration, which would also lead to a weaker SOI.

With the double (top and back) gated Hall bar samples for wafer A, the electrical transport properties (Hall sheet carrier density and mean free path) were varied by around ten percent. In figure 5, a linear dependence of l_{SO} on l_e is seen, just as we would expect for the EY mechanism, because spin relaxation is induced by scattering. Therefore, the DP mechanism (arising from Dresselhaus and Rashba SOI) seems to be negligible, as this would show a dependence of $l_{SO} \sim l_e^{-1}$, because spin precession is restarted by scattering [29,37].

The inset shows that as the external electric field is made more negative the SOI length becomes shorter, i.e. the SOI is becoming stronger. We interpret this negative dependence as another reason to disregard Dresselhaus SOI as a dominant factor in our samples, because this would be independent of changes in the local electric field. This is consistent with single InAs QWs, where the Dresselhaus term was responsible for less than 5 % of the SOI [38]. The strength of the Rashba SOI (structural or interface inversion symmetry) is theoretically predicted also to be controllable by a gate voltage, but previous experiments for InAs QWs did not provide a definite experimental confirmation of the sign of the correlation. They either did not vary carrier density [21] or did so by illumination with a light emitting diode, rather than applying a gate voltage [22]. Experiments with gate voltages either reported no gate dependence [23] or a negative dependence for top gate voltages [25]. For an inversion layer on *p*-type InAs, Schierholz et al. measured a positive dependence for SdH measurements and a negative dependence for values obtained from WAL [26,31]. Most recently Kim et al. found a negative or positive dependence determined by the QW potential gradient in accordance with theoretical predictions [20,27,39]. So the negative dependence we report here could be caused by DP with Rashba SOI or EY.

The inset in figure 5 shows the calculated band diagram of the heterostructure, we performed the calculation with nextnano³, a 3D Poisson and Schrödinger solver [40]. There is only a small positive difference in energy across the InAs layer of approximately 30 meV. It is unlikely that such a small gradient would cause Rashba SOI of the order we report here, and furthermore it would lead to a negative dependence of the SOI length. We also see a similar mobility dependence on gate voltage, so the most likely cause is scattering by impurities, particularly because we would expect a constant mobility for Rashba SOI [41].

To compare our reported SOI length values with the Rashba parameter from other experiments with InAs QWs, we used:

$$\alpha = \frac{\hbar^2}{m^* l_{SO}}$$

to calculate the SOI length for different sources. We note that there is a variance in the reported accompanying effective mass m^* . The results are presented in Table 1 and show that SOI length due to the EY mechanism is in the magnitude of the reported Rashba SOI lengths and cannot be neglected in a thorough investigation of spin relaxation mechanisms.

In conclusion, we report measurements of the spin-orbit interaction (SOI) in InAs/GaSb heterostructures using weak antilocalisation. We conclude that the dominant spin relaxation mechanism in the heterostructure reported here is the Elliott-Yafet mechanism and not inversion asymmetry effects (Dyakonov-Perel) as has been concluded previously and that the SOI is controllable by a gate voltage, which makes its application in spintronic devices possible. We also add to the ongoing discussion about gate controllable Rashba SOI by showing that a thorough experimental procedure has yet to be reported. To account for all spin relaxation mechanism the dependence of the SOI parameter on the mean free path, the gate voltage and the intrinsic carrier density have to be considered.

ACKNOWLEDGMENT

We acknowledge helpful discussions with S.F. Fischer and O. Chiatti. We also thank M. Rosamond for advice in all clean room work, J. Batley for assistance with low temperature measurements and G. Burnell for software support. This work was supported by the Engineering and Physical Sciences

Research Council, the EPSRC platform grant ‘Spintronics at Leeds’ (EP/M000923/1), the EPSRC National Centre for III-V Technologies and the Erasmus+ program (F. H.).

Author	Min. l_{SO} (nm)	m^*
Luo et al. [21]	154	0.055
Heida et al. [23]	317	0.040
Grundler et al. [25]	47	0.036
Schierholz et al. [26]	167	0.026
Kim et al. (2014) [27]	221	0.050
Kim et al. (2013) [20]	237	0.023
InAs/GaSb (this work)	150	-

Table 1: Comparison of the reported minimal SOI lengths derived from the largest spin splitting parameter α reported, calculated with the accompanying effective mass m^* .

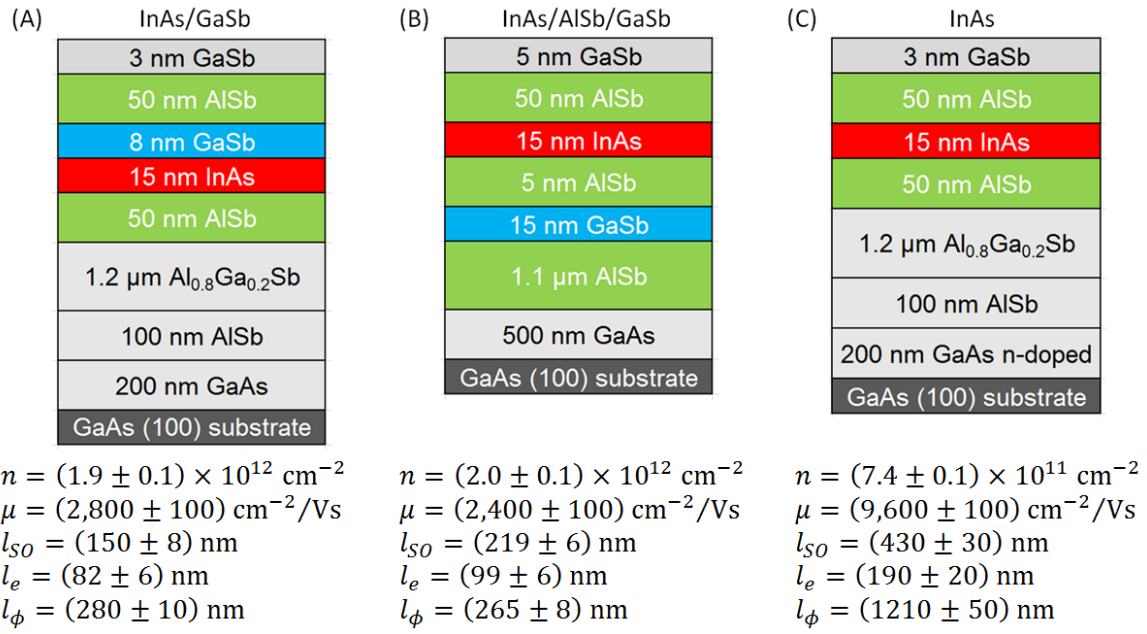


Figure 1: Comparison of the three wafers studied. The substrate is in all three cases n-doped, the InAs/GaSb wafer A has an interface doping with Si atoms of 10^{11} cm^{-2} . The charge carrier densities, mobilities and characteristic lengths are given at 1.7 K.

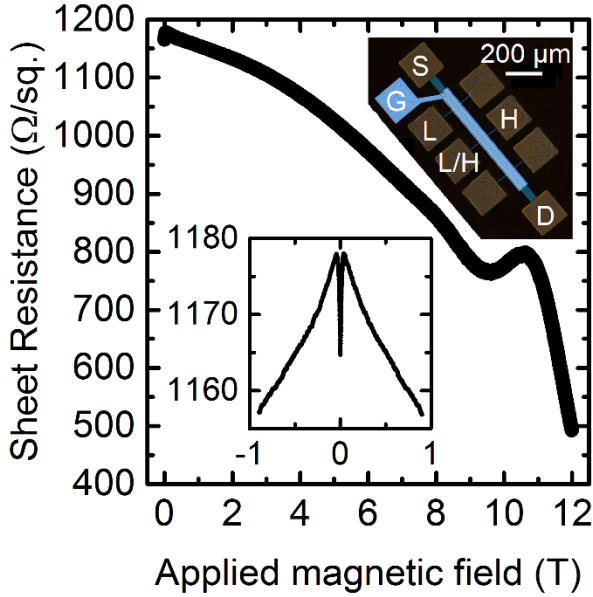


Figure 2: Magnetoresistance of an InAs/GaSb QW Hall bar sample (wafer A) at 340 mK and applied magnetic field of up to 12 T. Inset (top): Microscope image of the gated Hall bar geometry used here with labels for contacts (S = source, D = drain, G = gate, L = longitudinal voltage, H = Hall voltage). Inset (bottom): Low field magnetoresistance highlighting the WAL dip at zero field.

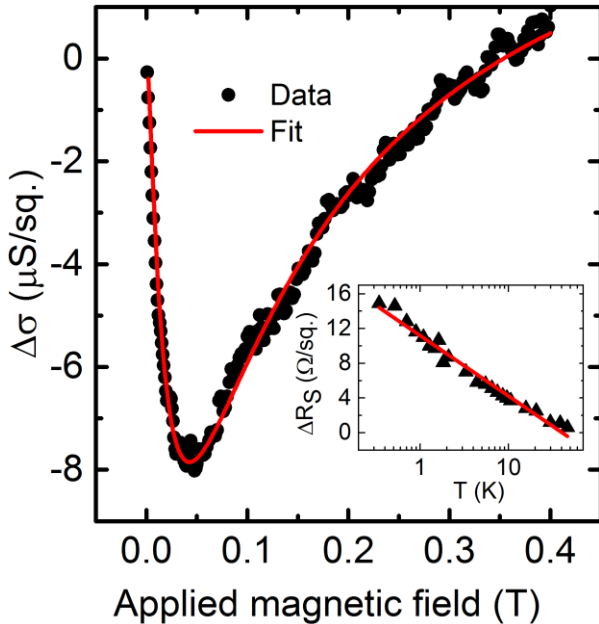


Figure 3: The change in conductivity for an InAs/GaSb QW Hall bar sample (wafer A) at 1.7 K as a function of perpendicular magnetic field. The black data points show the measured values, the red solid line shows the HLN-Fit with the following fit parameters: $l_{so} = 147$ nm, $l_e = 77$ nm and $l_\phi = 289$ nm. The fit and data match for the pictured low field range, for higher fields the background negative magnetoresistance leads to deviation from this behaviour and is excluded from the fit. Inset: The absolute change in sheet resistance for low fields as a function of temperature on a log scale. The black data points show the measured values, the red solid line shows a linear fit.

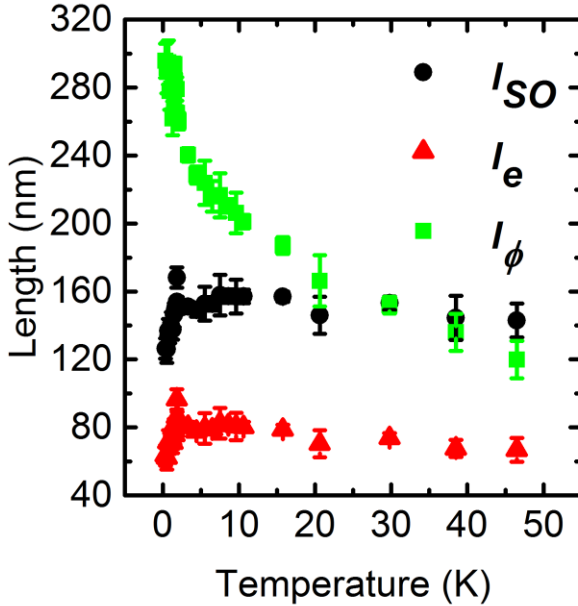


Figure 4: Characteristic lengths from the HLN fit as a function of temperature for the InAs/GaSb wafer (A). In agreement with the model WAL only occurs for temperatures where l_ϕ is of the order of l_{SO} or bigger (around 50 K, see also the inset in figure 3). The phase coherence lengths for wafers B and C are linear in temperature from 1.7 up to approximately 15 K, where they fall below the SOI length (which is, as well as l_e , almost temperature independent) and consequently no WAL is observable.

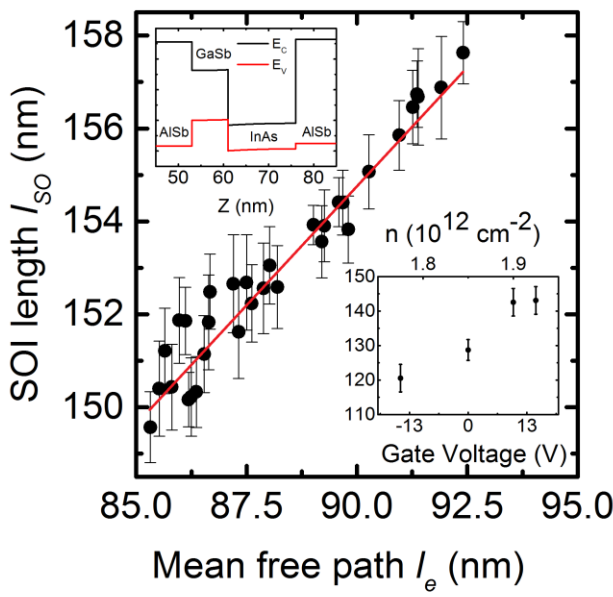


Figure 5: The SOI length as a function of the mean free path controlled by the Hall carrier density via an applied top gate voltage and back gate voltage for wafer A at 1.7 K.

Inset (top): Calculated band diagram showing the lowest conduction and the highest valence band energy, the band inversion inside the QW is also clearly evident. Inset (bottom): The SOI length as a function of the Hall carrier density controlled by an applied top gate voltage for wafer A at 340 mK.

- [1] M. Drndic, M. P. Grimshaw, L. J. Cooper, D. A. Ritchie, and N. K. Patel, *Applied Physics Letters* **70**, 481 (1997).
- [2] R. J. Wagner, B. V. Shanabrook, M. J. Yang, and J. R. Waterman, *Superlattices and Microstructures* **21**, 95 (1997).
- [3] M. J. Yang, C. H. Yang, B. R. Bennett, and B. V. Shanabrook, *Physical Review Letters* **78**, 4613 (1997).
- [4] T. P. Marlow, L. J. Cooper, D. D. Arnone, N. K. Patel, D. M. Whittaker, E. H. Linfield, D. A. Ritchie, and M. Pepper, *Physical Review Letters* **82**, 2362 (1999).
- [5] Y. Vasilyev, S. Suchalkin, K. von Klitzing, B. Meltser, S. Ivanov, and P. Kop'ev, *Physical Review B* **60**, 10636 (1999).
- [6] K. Suzuki, S. Miyashita, and Y. Hirayama, *Physical Review B* **67** (2003).
- [7] C. Petchsingh, R. J. Nicholas, K. Takashina, N. J. Mason, and J. Zeman, *Physical Review B* **70** (2004).
- [8] K. Nilsson, A. Zakharchova, I. Lapushkin, S. T. Yen, and K. A. Chao, *Physical Review B* **74** (2006).
- [9] C. Liu, T. L. Hughes, X. L. Qi, K. Wang, and S. C. Zhang, *Phys Rev Lett* **100**, 236601 (2008).
- [10] I. Knez, R. R. Du, and G. Sullivan, *Physical Review B* **81** (2010).
- [11] I. Knez, R. R. Du, and G. Sullivan, *Phys Rev Lett* **107**, 136603 (2011).
- [12] I. Knez, R. R. Du, and G. Sullivan, *Phys Rev Lett* **109**, 186603 (2012).
- [13] I. Knez, C. T. Rettner, S. H. Yang, S. S. Parkin, L. Du, R. R. Du, and G. Sullivan, *Phys Rev Lett* **112**, 026602 (2014).
- [14] C. Charpentier, S. Fält, C. Reichl, F. Nichele, A. Nath Pal, P. Pietsch, T. Ihn, K. Ensslin, and W. Wegscheider, *Applied Physics Letters* **103**, 112102 (2013).
- [15] F. Nichele, A. N. Pal, P. Pietsch, T. Ihn, K. Ensslin, C. Charpentier, and W. Wegscheider, *Phys Rev Lett* **112**, 036802 (2014).
- [16] E. M. Spanton, K. C. Nowack, L. Du, G. Sullivan, R. R. Du, and K. A. Moler, *Phys Rev Lett* **113**, 026804 (2014).
- [17] L. Du, I. Knez, G. Sullivan, and R. R. Du, *Phys Rev Lett* **114**, 096802 (2015).
- [18] V. S. Pribiag, A. J. Beukman, F. Qu, M. C. Cassidy, C. Charpentier, W. Wegscheider, and L. P. Kouwenhoven, *Nat Nanotechnol* **10**, 593 (2015).
- [19] T. Li *et al.*, *Phys Rev Lett* **115**, 136804 (2015).
- [20] K.-H. Kim, D.-S. Um, H. Lee, S. Lim, J. Chang, H. C. Koo, M.-W. Oh, H. Ko, and H.-j. Kim, *ACS Nano* **7**, 9106 (2013).
- [21] J. Luo, H. Munekata, F. F. Fang, and P. J. Stiles, *Physical Review B* **41**, 7685 (1990).
- [22] G. L. Chen, J. Han, T. T. Huang, S. Datta, and D. B. Janes, *Physical Review B* **47**, 4084 (1993).
- [23] J. P. Heida, B. J. van Wees, J. J. Kuipers, T. M. Klapwijk, and G. Borghs, *Physical Review B* **57**, 11911 (1998).
- [24] T. Koga, J. Nitta, T. Akazaki, and H. Takayanagi, *Phys Rev Lett* **89**, 046801 (2002).
- [25] D. Grundler, *Phys Rev Lett* **84**, 6074 (2000).
- [26] C. Schierholz, T. Matsuyama, U. Merkt, and G. Meier, *Physical Review B* **70**, 233311 (2004).
- [27] K. H. Kim, H. C. Koo, J. Chang, Y. S. Yang, and H. j. Kim, *IEEE Transactions on Magnetics* **50**, 18 (2014).
- [28] C. Brüne, A. Roth, H. Buhmann, E. M. Hankiewicz, L. W. Molenkamp, J. Maciejko, X.-L. Qi, and S.-C. Zhang, *Nature Physics* **8**, 486 (2012).
- [29] P. D. Dresselhaus, C. M. Papavassiliou, R. G. Wheeler, and R. N. Sacks, *Phys Rev Lett* **68**, 106 (1992).
- [30] R. J. Elliott, *Physical Review* **96**, 266 (1954).
- [31] T. Matsuyama, R. Kürsten, C. Meißner, and U. Merkt, *Physical Review B* **61**, 15588 (2000).
- [32] C. Morrison, J. Foronda, P. Wiśniewski, S. D. Rhead, D. R. Leadley, and M. Myronov, *Thin Solid Films* **602**, 84 (2016).
- [33] S. Hikami, A. I. Larkin, and Y. Nagaoka, *Progress of Theoretical Physics* **63**, 707 (1980).
- [34] G. Bergmann, *Physics Reports* **107**, 1 (1984).
- [35] G. Dumpich and A. Carl, *Physical Review B* **43**, 12074 (1991).
- [36] F. Nichele, Kjaergaard, M., Suominen, H.J., Skolasinski, R., Wimmer, M., Nguyen, B.M., Kiselev, A.A., Yi, W., Sokolich, M., Manfra, M.J. and Qu, F., arXiv preprint, arXiv:1605.01241 (2016).
- [37] I. Žutić, J. Fabian, and S. Das Sarma, *Reviews of Modern Physics* **76**, 323 (2004).
- [38] Y. Ho Park, H.-j. Kim, J. Chang, S. Hee Han, J. Eom, H.-J. Choi, and H. Cheol Koo, *Applied Physics Letters* **103**, 252407 (2013).
- [39] K.-H. Kim, H.-j. Kim, H. C. Koo, J. Chang, and S.-H. Han, *Applied Physics Letters* **97**, 012504 (2010).
- [40] S. Birner, T. Zibold, T. Andlauer, T. Kubis, M. Sabathil, A. Trellakis, and P. Vogl, *IEEE Transactions on Electron Devices* **54**, 2137 (2007).
- [41] X.-J. Hao *et al.*, *Nano Letters* **10**, 2956 (2010).